ACS APPLIED MATERIALS & INTERFACES
Research Article
www.acsami.org

Investigating Zigzag Film Growth Behaviors in Layer-by-Layer Self-Assembly of Small Molecules through a High-Gravity Technique

Mengjiao Cheng, Chao Jiang, Caijun Luo, Yajun Zhang, and Feng Shi*

State Key Laboratory of Chemical Resource Engineering & State Key Laboratory of Organic−Inorganic Composites, Beijing University of Chemical Technology, Beijing, China

Supporting Information

ABSTRACT: The zigzag film growth behavior in the layer-by-layer (LbL) assembly method is a ubiquitous phenomenon for which the growth mechanism was rarely investigated, especially for small molecules. To interpret the zigzag increasing manner, we hypothesized that the desorption kinetics of small molecules was dominant for the film growth behavior and demonstrated this hypotheis by introducing the high-gravity technique into the LbL assembly of a typical polyelectrolyte/small molecule system of polyethylenimine (PEI) and meso-tetra(4-carboxyphenyl)porphine (Por). The results showed that the high-gravity technique remarkably accelerated the desorption process of Por; the high-gravity LbL assembly provides a good platform to reveal the desorption kinetics of Por, which is tedious to study in conventional situation. We found that as much as 50 min is required for Por molecules to reach desorption equilibrium from the substrate to the bulk PEI solution for the conventional dipping method; however, the process could be accelerated and require only 100 s if a high-gravity field is used. Nonequilibrated desorption at 10 min for normal dipping and at 30 s for high-gravity-field-assisted assembly both exhibited a zigzag film growth, but after reaching desorption equilibrium at 100 s under a high-gravity field, film growth began to cycle between assembly and complete disassembly instead of LbL assembly. For the first time we have proven that the high-gravity technique can also accelerate the desorption process and demonstrated the desorption-dependent mechanism of small molecules for zigzag film growth behaviors.

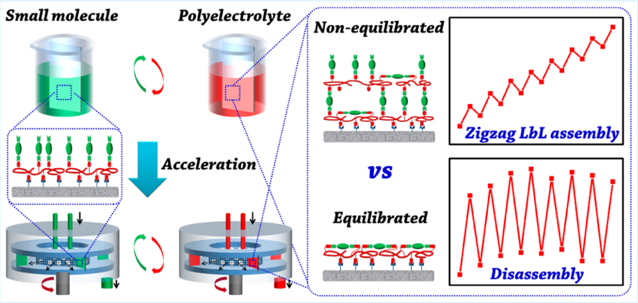

KEYWORDS: *layer-by-layer assembly, small molecule, zigzag increasing, high gravity, desorption*

INTRODUCTION

Incorporating small molecules such as metal ions, dyes, and drug molecules into layer-by-layer (LbL) assembled multilayers is important for various applications in catalysis,[1−3] nanocontainers and reactors,[4,5] microcapsules,[6] drug delivery,[7,8] flame-retardants,[9] and so on. Currently, there are three important strategies used to load small molecules into the multilayer during the LbL process: grafting targeted small molecules onto polyelectrolytes for subsequent LbL assembly,[10−13] direct assembly of small molecules as building blocks with counter polyelectrolytes,[1,14−17] and preassembling small molecules and polyelectrolytes to form a complex building block for further LbL assembly.[18−20] Compared with the pre-chemical-grafting method, the latter two methods are better suited to incorporate small molecules into the multilayer through noncovalent interactions. However, the noncovalent interaction always leads to a common phenomenon in which the film growth displays a zigzag increasing pattern.[21−30] The pattern is visible when observing the LbL assembled multilayer through UV−visible spectra, especially when small molecules are directly used as building blocks.[1,14−17,30] The zigzag increasing pattern indicates that when a substrate that has had its outermost layer modified with small molecules is immersed into a polyelectrolyte solution, the small molecules undergo desorption or extraction to some degree.[10−20] This results in a decrease in the absorbance of the multilayer with polyelectrolyte at the outermost layer versus that of the film with small molecules at the outermost layer. It is reported in the literature that the zigzag film increasing can be interpreted in two ways. For the LbL process involving small molecules, one hypothesis attributes the reduced amount of small molecules to the competitive balance between adsorption of the counter polyelectrolyte onto the substrates and dissolution of the small molecules into the polyelectrolyte solutions.[24−30] For this case, it is concluded that when the polyelectrolyte reached a saturated adsorption on the substrate, the desorption of the small molecules also reached equilibrium. For the LbL assembly of polyelectrolytes, the second hypothesis interprets the increasing−decreasing zigzag phenomena with a change in the hydrated water content.[22,23,31] However, the mechanism for the zigzag growing pattern in an LbL assembly that directly uses small molecules as the building blocks, specifically, the desorption of small molecules, has rarely been investigated. For this study, we used a typical polyelectrolyte, polyethyleni-

Received: June 22, 2015
Accepted: August 10, 2015
Published: August 10, 2015

DOI: 10.1021/acsami.5b05555
ACS Appl. Mater. Interfaces 2015, 7, 18824−18831

Scheme 1. Illustration of the Desorption-Dominant Mechanism of Zigzag Film Growth or Cycled Assembly/Disassembly

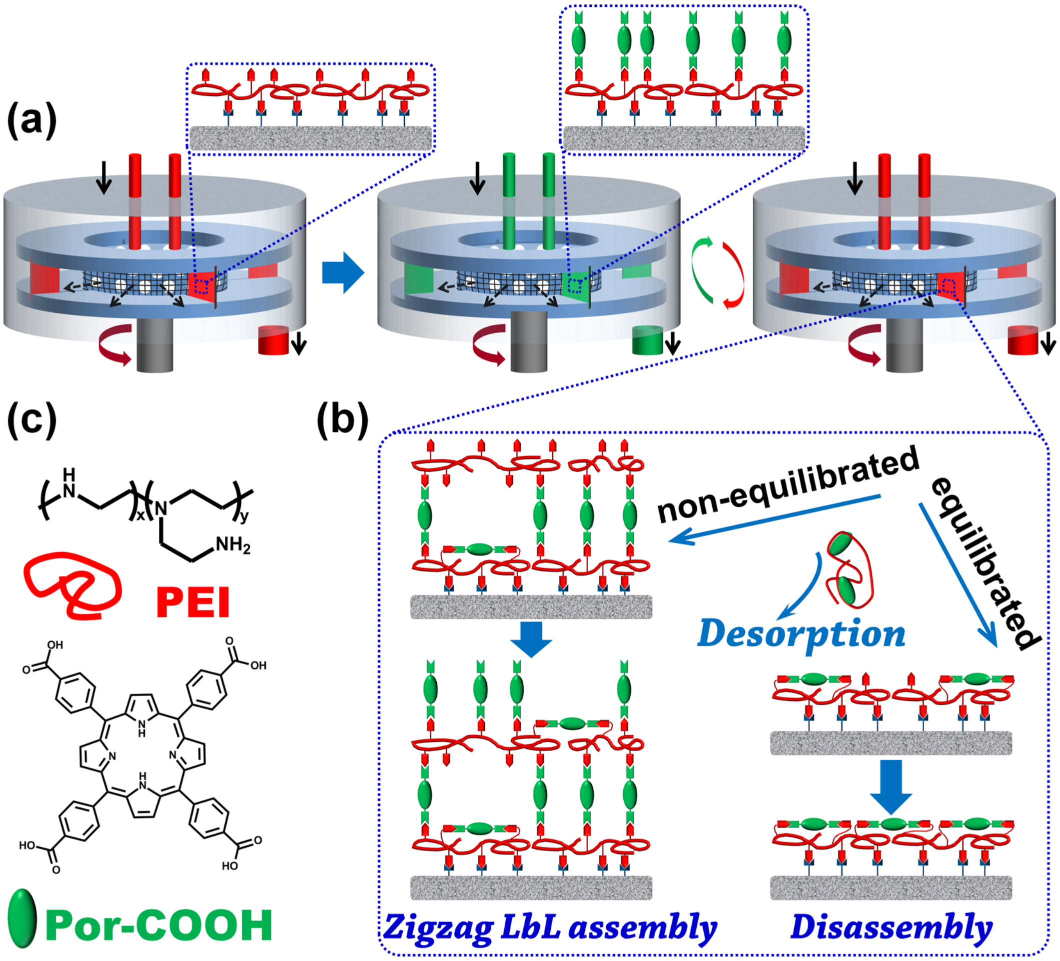

mine (PEI), and a small molecule, meso-tetra(4-carboxyphenyl)porphine (Por), as model building blocks to construct a multilayer; the Por molecule was reportedly useful in tuning self-assembly behaviors to achieve unique optical and catalytic properties.[32,33] The film growth behaviors of PEI/Por multilayers and the desorption of Por in the presence of PEI are used to investigate the mechanism of their zigzag growing patterns.

Because the desorption of Por is a time-consuming procedure, we introduced the well-established process intensification technique of a high-gravity field[34] into the LbL assembly of the PEI and Por. Although the high-gravity field has been shown to accelerate the adsorption process in LbL assembly more than conventional dipping,[35−38] this is the first time it has been demonstrated that the high-gravity technique can also accelerate the desorption process. We found that as much time as 50 min is required for Por molecules to reach desorption equilibrium from the substrate to the bulk PEI solution for the conventional dipping method; however, the process could be accelerated and require only 100 s if a high-gravity field is used. Nonequilibrated desorption both at 10 min for normal dipping and at 30 s for high-gravity-field-assisted assembly exhibited a zigzag film growth. However, after reaching desorption equilibrium at 100 s under a high-gravity field, the film growth began to cycle between assembly and complete disassembly. Therefore, we propose the hypothesis that the zigzag film growth might be attributed to the incomplete desorption of the small molecules into the polyelectrolyte solution, therefore not reaching desorption equilibrium and leading to the decreased absorbance of the small molecules in the PEI solution and subsequent increased absorbance by readsorption in the Por solution. When the Por reaches desorption equilibrium, the absorbance of Por decreases because of its complete disassembly into the PEI solution, and readsorption of the Por occurred again after being exposed to the Por solution again, contributing to an assembly/disassembly cycle (Scheme 1). Hence, LbL assembly using a high-gravity field is not only an efficient strategy to accelerate the tedious LbL process it also provides a platform for investigating the mechanism for the observed zigzag film growth, specifically for the LbL assembly of small molecules.

■ EXPERIMENTAL SECTION

Materials and Instrument. The following chemicals were used as supplied: PEI (branched, MW 1800) from Acros Organics; Por from Sigma-Aldrich; H_2SO_4 (98%), H_2O_2 (30%), and ethanol from Sinopharm Chemical Reagent Beijing Co. (Beijing, China). The UV−visible spectra were obtained on a Hitachi U-3900H spectrophotometer. Atomic force microscopy (AFM) images were obtained on a Dimension 3100 instrument from Veeco.

The high-gravity machine for LbL assembly was homemade as illustrated in Scheme S1: the inner diameter of the rotator is 20 mm and the outer diameter 50 mm. The internal and external widths of the rotator are 10 mm and 17 mm, respectively. Four slots (14 mm × 12 mm × 1 mm) are set in four directions inside the rotator. The distributor consists of two pipes (5 mm × 1 mm), with each having a

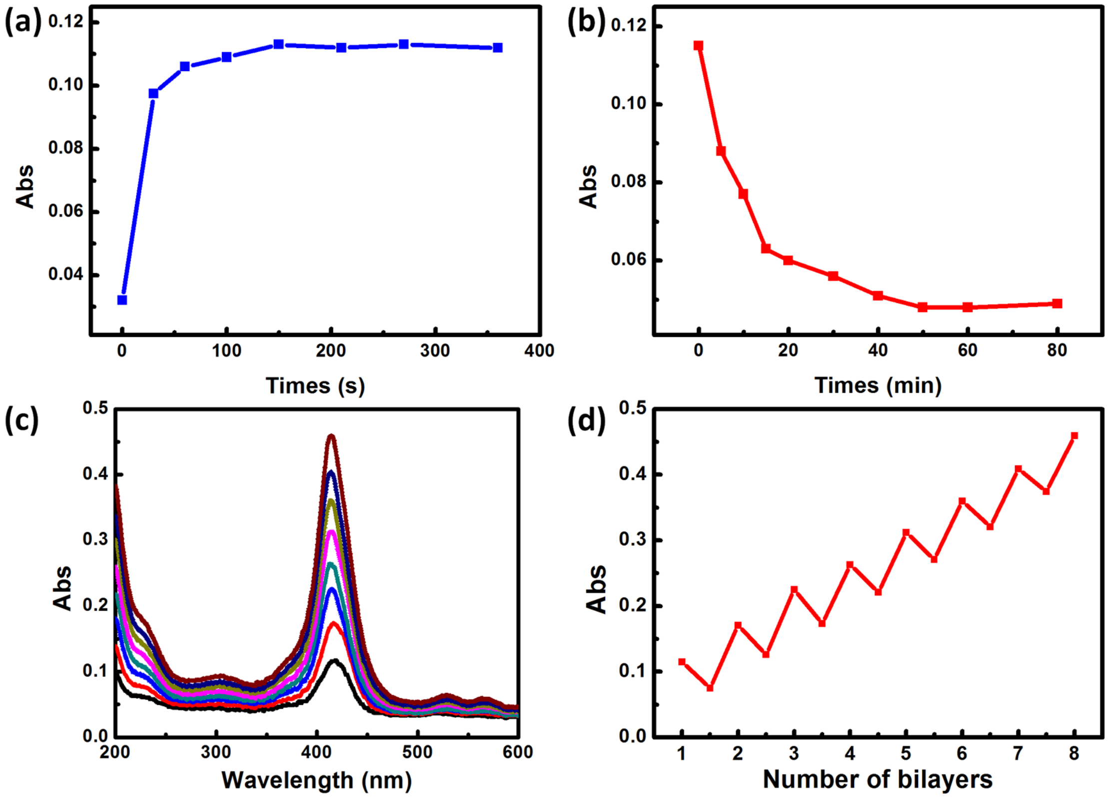

Figure 1. (a) Adsorption kinetics of Por deposited on quartz substrate premodified with a layer of PEI. (b) Desorption kinetics of a $(PEI/Por)_1$ layer when exposed to PEI solution for different time intervals. (c) UV−visible spectra of the zigzag film growth (nonequilibrated desorption) of the $(PEI/Por)_n$ multilayer (n = 1, 2, ..., 8) under dipping method. (d) Correlation of Por absorbance at 425 nm versus each single layer number in (c).

hole of 1 mm diameter. The rotator is installed inside the fixed cavity with a diameter of 100 mm and rotates at the speed of several hundreds to thousands of revolutions per minute. The polyelectrolyte solutions are pumped into the cavity using a peristaltic pump (BT100-2J) from Baoding Longer Precision Pump Co., Ltd.

Pretreatment of Substrates. The quartz substrates or silicon wafers used in all experiments were cleaned using a piranha solution, which was a mixed solution of H_2SO_4 (wt 98%) and H_2O_2 (wt 30%) with a volume ratio of 7:3 at room temperature. Afterward, the substrates or wafers were rinsed with deionized water and dried in a nitrogen flow. It should be noted that the piranha solution is extremely corrosive and should be used in a fume hood and handled with acid-resistant gloves.

Adsorption Kinetics of Por under Conventional Dipping Assembly. The cleaned quartz substrates were immersed in a PEI ethanol solution (1 mg/mL) for 30 min to ensure the saturated adsorption of the polyelectrolyte, followed by rinsing in copious amounts of ethanol and drying in a nitrogen flow. Then, the substrates with a layer of PEI were transferred to a Por ethanol solution (0.01 mg/mL). After immersion in the Por solution for a given time interval ranging from 30 s to 6 min, the substrates were washed with ethanol and dried in a nitrogen flow, and the adsorbed amount of Por was detected by UV−visible spectra. For each time interval, three substrates were used, following identical experimental conditions, to give an averaged adsorption amount. The correlation of absorbance versus corresponding adsorption time was plotted to give adsorption kinetics.

LbL Assembly of PEI and Por by Using Normal Dipping Method. First, the cleaned quartz substrates were immersed in a PEI ethanol solution (1 mg/mL) for 30 min as the first layer, rinsed in ethanol, and dried in a nitrogen flow. Second, the substrates were deposited in a Por ethanol solution (0.01 mg/mL) for 10 min, followed by washing with ethanol and drying in N_2. Third, the substrate was alternately immersed in a PEI solution (ethanol, 1 mg/mL) for 10 min (nonequilibrated desorption) or 50 min (equilibrated desorption) and a Por solution (ethanol, 0.01 mg/mL) for 10 min, between which the substrates were rinsed and dried. After deposition of each single layer of either PEI or Por, the substrates were characterized with UV−visible spectra.

Adsorption Kinetics of Por under High-Gravity Field. The cleaned quartz substrates were immersed in a PEI ethanol solution (aq, 1 mg/mL) for 30 min under normal dipping conditions, followed by washing with ethanol and drying in a nitrogen flow. Subsequently, the substrates with a layer of PEI were inserted into slots on the rotator of the high-gravity machine; the Por ethanol solution (0.01 mg/mL) was continuously pumped through a peristaltic pump into the machine at a flowing rate of 30 mL/min. The pumped liquid entered the machine from the inlet, passed through the packing layer around the center axis of the rotator, and flowed through the substrates, which were fixed close to the packing layer in the radial direction with their largest surface vertical to the rotator axis. The immersion time was counted as the time when the Por solution was pumped in and the rotator reached a required rotating speed of 2400 rpm. After deposition in Por under a high-gravity field for a given time interval, the substrates were rinsed by pumping ethanol into the high-gravity equipment for 1 min and dried by allowing the machine to continue rotating for 1 min without anything being pumping in. Afterward, the substrates were removed from the high-gravity machine and characterized with UV−visible spectra. The adsorption kinetics of Por onto PEI were determined by correlating the absorbance with the corresponding adsorption time.

LbL Assembly of PEI and Por under High-Gravity Field. First, the cleaned quartz substrates were immersed in PEI solution (ethanol, 1 mg/mL) for 30 min as the first layer, rinsed in deionized water, and dried in nitrogen flow. Second, the substrates were inserted into the slots of the high-gravity equipment, and Por solution (ethanol, 0.01 mg/mL) was continuously pumped in for 30 s (nonequilibrated desorption) or 100 s (equilibrated desorption). The substrates were washed by pumping deionized water into the high-gravity equipment for 1 min and dried by keeping the machine rotating for 1 min without anything being pumping in. Third, the PEI solution (ethanol, 1 mg/

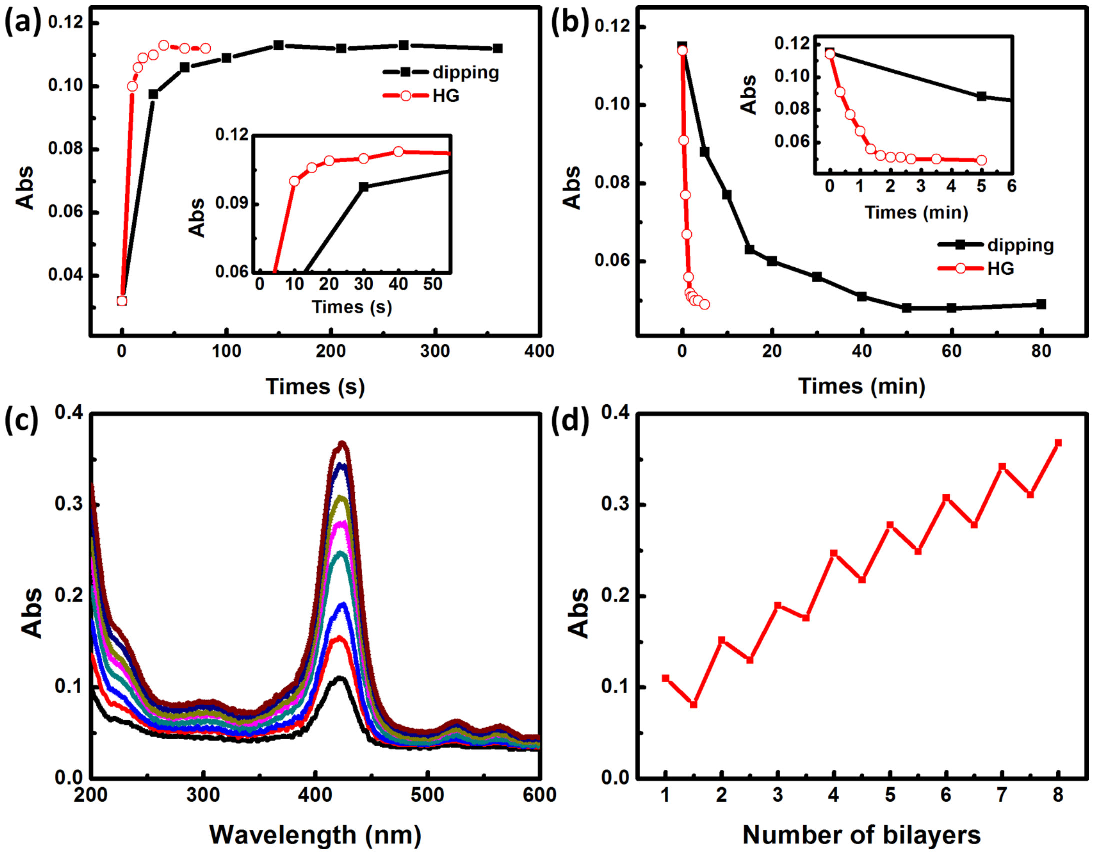

Figure 2. (a) Adsorption kinetics of Por under high-gravity field (red circles) and dipping method (black squares). (b) Desorption kinetics of a $(PEI/Por)_1$ layer in PEI solution under high-gravity field (red circles) and dipping method (black squares). The insets in panels a and b are corresponding local magnified curves with a short time interval. (c) UV−visible spectra of the zigzag film growth (nonequilibrated desorption) of the $(PEI/Por)_n$ multilayer (n = 1, 2, ..., 8) under high-gravity field. (d) Correlation of Por absorbance at 425 nm versus each single layer number under high-gravity field in (c).

mL) and Por solution (ethanol, 0.01 mg/mL) were alternately pumped into the high-gravity machine for 1 min and 30 or 100 s, respectively, between which the substrates were rinsed and dried. After deposition of each single layer in either PEI or Por, the substrates were characterized with UV−visible spectra.

■ RESULTS AND DISCUSSION

Adsorption Kinetics of Por. We demonstrate the above hypothesis using a model system of PEI (with rich amino groups) and Por (a small molecule with four carboxylic acid groups) for LbL assembly driven by hydrogen bonding. Generally, in LbL assembly, the immersion time for the building block is determined by the adsorption kinetics, in which the deposition time was used after reaching saturated adsorption. The adsorption kinetics of the Por was determined by immersing the quartz substrate, which was modified with a layer of PEI, in an ethanol solution of Por (0.01 mg/mL) at different time intervals using the conventional dipping method. After immersion at each time interval, a UV−visible spectrum at 425 nm was used to determine the extent of deposition onto the Por. The absorbance values for the Por at 425 nm were correlated with the corresponding immersion time, which revealed the adsorption kinetics of Por. As shown in Figure 1a, the adsorption of Por molecules rapidly increased in the first 30 s, then slowed, and reached a constant value after 150 s, indicating a saturated adsorption of Por. For the Por to reach saturated adsorption, it was determined that 10 min of deposition time in the Por solution was necessary for its subsequent use in the LbL assembly process with PEI.

Zigzag Film Growth of LbL Assembled PEI/Por Multilayer. The LbL assembly of $(PEI/Por)_n$ multilayers (n refers to the cycled number of the alternate immersion in PEI and Por) was achieved by alternately immersing the substrates into a PEI ethanol solution (1 mg/mL) for 20 min and into a Por ethanol solution (0.01 mg/mL) for 10 min. After each cycle of dipping, the substrate was rinsed with ethanol, dried in a nitrogen flow, and characterized using UV−visible spectra. The stepwise UV−visible curve for each layer of the $(PEI/Por)_n$ multilayer is shown in Figure 1c, and the expected zigzag film growth is observed. When Por was in the outermost position for a bilayer, the absorbance versus deposited number of bilayers showed a regular linear increase, suggesting that an identical amount of Por was deposited during each cycle (Figure 1d). However, when PEI was in the outermost position for the bilayer, the UV−visible absorbance decreased to 63% of the value of the multilayer when Por was in the outermost position prior to immersion in the PEI. After subsequent immersion in the Por solution, the absorbance value again increased. The absorbance difference between a multilayer with Por in the outermost position and one with PEI in the outermost position remained constant, thus contributing to another linear correlation between the absorbance of $(PEI/Por)_{n.5}$ multilayers and the number of half bilayers. For clarity, the UV−visible spectra for the $(PEI/Por)_n$ multilayers (n = 1, 2, 3, ..., 8) were overlaid in Figure 1c, and we observed the

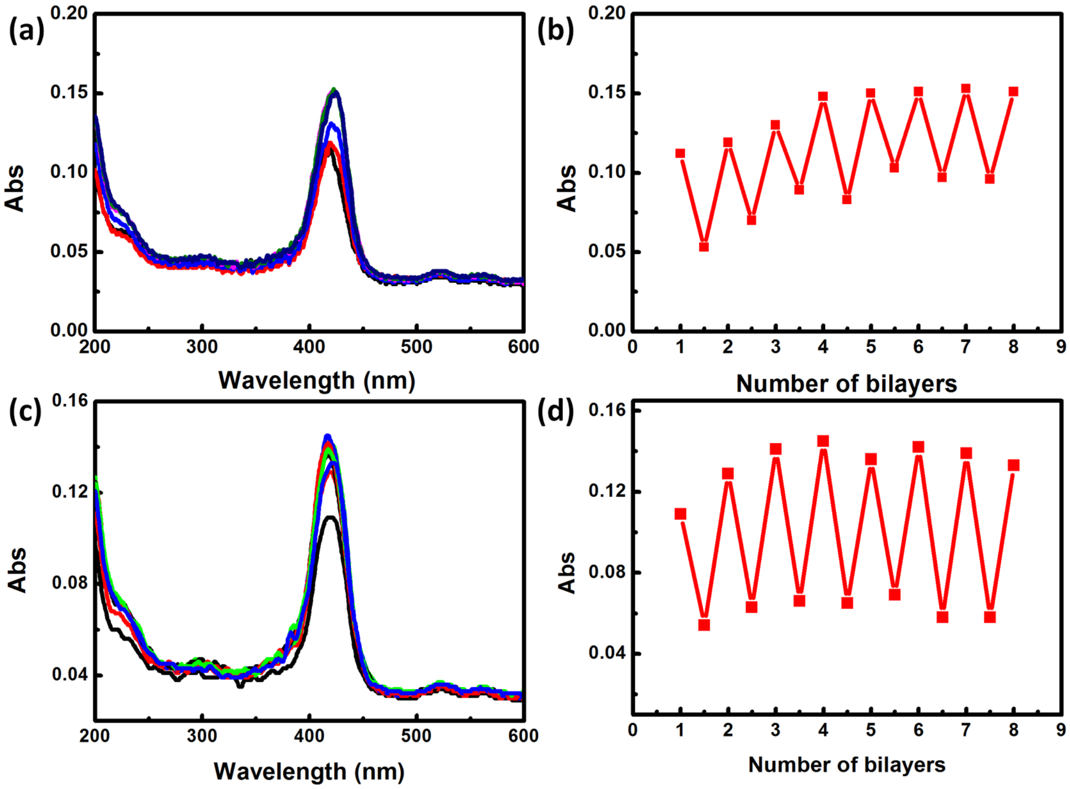

Figure 3. (a) UV−visible spectra of PEI/Por multilayer (equilibrated Por desorption) under high-gravity field with desorption time of 100 s. (b) Correlation of absorbance at 425 nm versus number of each single cycle of PEI/Por in (a). (c) UV−visible spectra of PEI/Por multilayer (equilibrated Por desorption) under conventional dipping method with desorption time of 50 min. (d) Correlation of Por absorbance at 425 nm versus each single cycle of PEI/Por in (c).

homogeneous increase in the absorbance value for each bilayer, from which it is inferred that the deposited amount of Por in each bilayer was identical. This kind of zigzag film growth was ubiquitous in the field of LbL assembly, especially for an LbL process containing small molecules. Many studies assumed that the small molecules were extracted or partially desorbed from the substrate to the solution, thus resulting in a zigzag growing film. Generally, it was hypothesized that, during the process when the substrate was immersed in the polyelectrolyte solution, the desorption of small molecules from the substrate to solution should have reached equilibrium, indicating that the desorption of the small molecules was complete. There is little research in the literature that explores the desorption kinetics for the exposure of adsorbed small molecules to polyelectrolyte solutions.

Desorption Kinetics of Por Exposed to PEI Solution. To determine whether the desorption of Por has reached equilibrium, the desorption kinetics of Por in the presence of a PEI solution are investigated by immersing the substrate with a $(PEI/Por)_1$ layer into a PEI solution for different time intervals. Next, the Por content on the substrate is detected using the UV−visible spectra. From Figure 1b, it is observed that after exposure to the PEI solution for 10 min, the Por absorbance decreased to 68% of the original value before immersion in the PEI solution. Desorption continued with increasing immersion time in the PEI and reached a constant value after 50 min. On the basis of the desorption kinetics, the zigzag film growth could be explained. When the deposition time of the PEI was <50 min, which is not long enough for Por to reach deposition equilibrium, the Por absorbance on the substrate after immersion in the PEI solution might not decrease to its minimum. However, after readsorption in the subsequent Por solution, the Por absorbance value should increase again, therefore resulting in a zigzag absorbance growth pattern of alternate reduction−increase. If the PEI deposition time exceeds 50 min to achieve desorption equilibrium, a majority of the Por molecules could desorb from the substrate into the PEI solution; therefore, very little of the PEI would be deposited onto the substrate, leading to a minimal increase in Por absorbance for subsequent deposits in the Por solution. The 50 min immersion time for a single layer and 50 min or longer time for the deposition of each layer is extremely time-consuming. Therefore, it is difficult to observe the desorption kinetics of small molecules, and in addition to the time required to reach desorption equilibrium, LbL assembly becomes a tedious process.

Adsorption and Desorption Kinetics of Por under High-Gravity Field. We considered whether an accelerated high-gravity-field-assisted LbL assembly method would shorten the required time for equilibrium, thus providing a simple technique for investigating the zigzag film growth mechanism. The high-gravity technique is known as an efficient method of process intensification in chemical engineering[34] and is accomplished by rapid rotation to produce a high acceleration rate, vigorous turbulent flow, and strong shear stresses to dramatically enhance mass or heat transfer. To investigate LbL assembly of PEI/Por under high gravity, first, the adsorption kinetics of Por in a high-gravity field was studied to determine the required LbL deposition time. A quartz substrate deposited with a layer of PEI was fixed onto a high-gravity rotator, through which the Por solution was continuously pumped for various time intervals. The adsorption kinetics of Por

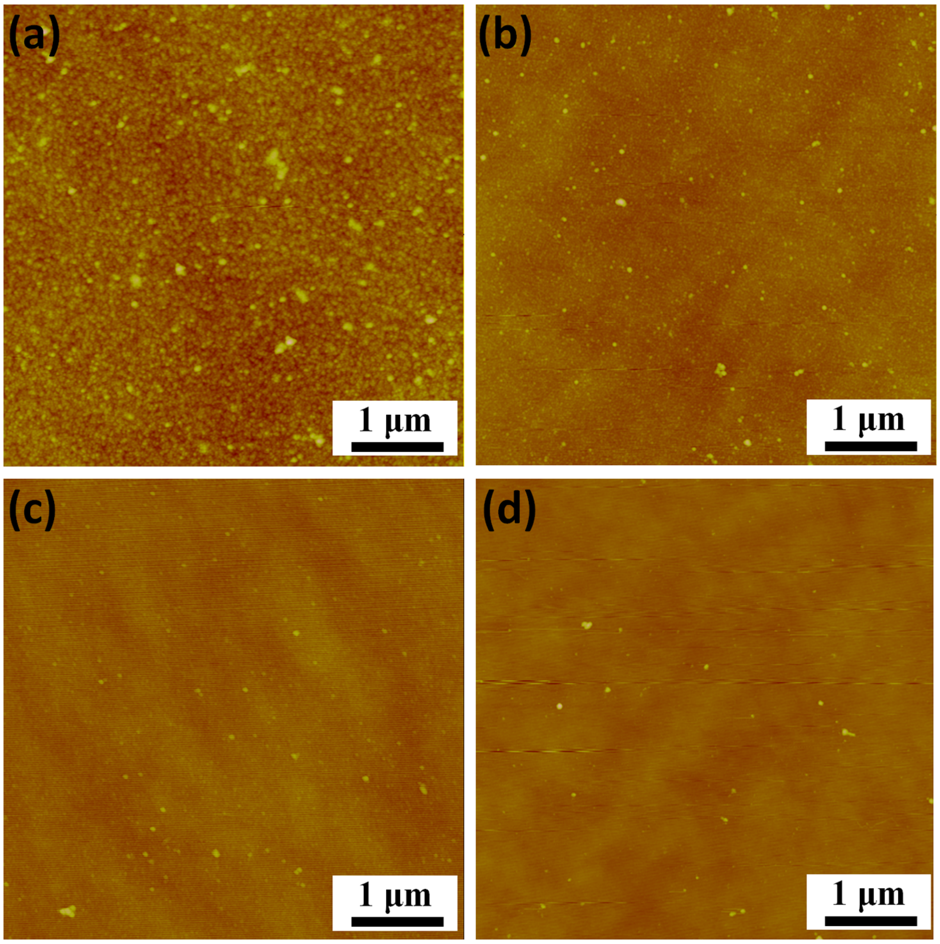

Figure 4. When Por desorption equilibrium was not reached, AFM images of the zigzag growing PEI/Por multilayers fabricated under (a) dipping method and (b) high-gravity field showed surface roughness values of 2.3 and 1.4 nm, respectively. When desorption of Por reached equilibrium, the AFM images of films prepared under (c) dipping method and (d) high-gravity field indicate surface roughness values of 1.4 and 0.9 nm, respectively.

absorbance versus deposition time is shown in Figure 2a. It was observed that the time to reach saturated adsorption was shortened remarkably from 150 s for the conventional dipping method to 40 s using a high-gravity field. However, the saturated adsorption content of the Por was somewhat similar to that obtained from the conventional dipping method. Hence, the high-gravity field enhanced the film deposition rate without disturbing the chemical equilibrium. An approximate 4-fold increase in the adsorption process was verified by our previous work.[35] The reason for the acceleration effect of the high-gravity field is that the strong shear stresses and the highly turbulent flow reduce the thickness of the diffusion layer, decreasing the resistance to mass transfer and thus promoting the diffusion and adsorption of Por. To gain a better understanding of the desorption kinetics that determine zigzag film growth, it is important to study the desorption kinetics of Por in a PEI solution while under a high-gravity field. Therefore, a quartz substrate was prepared with a fixed $(\mathrm{PEI}/\mathrm{Por})_1$ layer in the high-gravity equipment, and a PEI solution was continuously pumped for a certain time interval. The absorbance of the Por decreased rapidly within 1 min, and the desorption equilibrium was reached in 100 s, which was much faster than that for conventional dipping (50 min). This result demonstrated that the high-gravity field was effective in accelerating the desorption process of small molecules in an LbL assembly by as much as 30-fold. Similarly, we attributed the rapid desorption of the Por to the thinned boundary layer that exists when under a high-gravity field, through which the desorbed Por diffused into solution.

LbL Assembly of Por under Nonequilibrated and Equilibrated Desorption of Por. Because the high-gravity field showed remarkable acceleration effects for both Por adsorption and desorption, we turned our attention to examining the proposed hypothesis by investigating the LbL assembly of a PEI/Por multilayer under a high-gravity field for the nonequilibrated and equilibrated desorption of Por. The PEI solution (ethanol, 1 mg/mL) and the Por solution (ethanol, 0.01 mg/mL) were alternately pumped into the high-gravity machine, and the equipment was continuously rotated in the presence of the solutions for 1 min and 30 s, respectively. Between each deposition step, ethanol was pumped for washing, followed by drying through rotating while nothing is pumped in. It was found that, prior to reaching desorption equilibrium after a 30 s deposition time, the film growth followed a zigzag pattern similar to what is seen in the LbL assembly process when conventional dipping is used. The absorbance when PEI was the outermost layer and when Por was the outermost layer displayed a linear correlation with the corresponding number of layers. After extending the deposition time in PEI from 30 to 100 s for the equilibrated desorption of Por, the Por absorbance versus each single layer exhibited a cycled assembly/disassembly behavior (Figure 3a,b) instead of a zigzag growing film. Most of the absorbance values of (PEI/Por)$_{n.5}$ remained at approximately the same level, which was comparable to that of (PEI/Por)$_1$.

The reason for the cycled assembly/disassembly was attributed to the following facts: when the substrate deposited with PEI was immersed into the Por solution, Por was absorbed onto the surface driven by the hydrogen bonding between PEI and Por. When the adsorption of Por reaches equilibration, the functional groups on the substrate should transfer from amino groups on PEI to carboxylic acid groups on Por. This phenomenon is the basis for the realization that in the formation of LbL assembled multilayers after each layer, the functional groups on the surface should be reversed. When the substrate with one bilayer of PEI/Por is transferred into the PEI solution, the PEI molecules should deposit onto the substrate by interacting with the excessive Por molecules, as illustrated in Scheme 1 (nonequilibrated); simultaneously, excessive PEI molecules formed a complex with Por molecules to result in the desorption of Por from the substrate, leading to a drop in Por absorbance. After reaching desorption equilibrium, the Por molecules oriented with the conformation that there is no excessive PEI, as illustrated in Scheme 1 (equilibrated). In this way, the original excessive Por molecules were thoroughly desorbed and only one bilayer of PEI/Por remained on the surface in the cycled immersion in PEI and Por solutions. The mechanism of LbL assembly being dependent on the desorption equilibrium also supported LbL assembling behaviors using the conventional dipping method: once the desorption time was sufficient to reach equilibrium (50 min), the LbL assembly also experienced a cycled assembly/disassembly pattern (Figure 3c,d).

Surface Morphology of the Por Multilayer. To further confirm the hypothesis of varied film growth caused by either the equilibrated or nonequilibrated desorption of Por, we characterized the film morphology through AFM images of the assembled multilayer for the conventional dipping method and for a high-gravity field. The zigzag growing PEI/Por multilayer was prepared for a 10 min deposition time in PEI (i.e., the desorption time of Por was 10 min for nonequilibrated desorption). The surface had a relatively smooth morphology with homogeneous and closely packed aggregates accompanied by a few large accumulations, leading to a surface roughness of approximately 2.3 nm (Figure 4a). The surface morphology was typical for a polyelectrolyte-containing multilayer, on which the aggregates were entanglements of polymers. For the interval far less than the time required to reach equilibrium, the multilayer would grow in a zigzag fashion, contributing to full coverage and a relatively high surface roughness. When subjected to a high-gravity field, at 10 s of nonequilibrated Por adsorption, the zigzag film grew, and the surface of the zigzag growing PEI/Por multilayer was smoother with a lower surface roughness of 1.4 nm (Figure 4b). Additionally, the surface was more compact than that fabricated by dipping at a similar Por desorption state. This result corresponded well with previous results,[37] showing that the strong shear forces produced under a high-gravity field partially removed the rough aggregates formed on the substrates at the nanoscale, leading to a smoother and more compact film. This is because the high-gravity field generated a highly turbulent flow, which diminished the boundary layer to the nanoscale; therefore, the formed rough or loosely packed structures would be destroyed by fluidic impact or shear. Moreover, the lower roughness of the zigzag growing PEI/Por multilayer under a high-gravity field supports a lower Por absorbance under high gravity when compared with that prepared by the normal dipping method at the same layer (Figures 1d and 2d). This is because the rough structures might increase light capture within the structure when characterized with UV−visible spectra, thus leading to high absorbance values. When the multilayer was assembled at an equilibrated Por desorption time of 100 s, the surface roughness decreased to a minimum of 0.9 nm (Figure 4d). Similarly to the multilayer fabricated under conventional dipping method (Figure 4c), we can observe that there are few randomly scattered aggregates, and the surface appearance is close to a blank substrate. This phenomenon supports the hypothesis that after desorption equilibrium is reached, there should be little film growth but only assembly or disassembly of one PEI/Por bilayer, for which the film should be thin and sparse. The film morphology in this situation matched well with the low absorbance of the Por in UV−visible spectra in Figure 3.

■ CONCLUSION

In summary, we have investigated and interpreted the mechanism for zigzag film growth during the LbL assembly of a PEI/Por multilayer by introducing a high-gravity field to study the adsorption/desorption kinetics of Por. We found that the zigzag film growth was caused by the nonequilibrated desorption of Por when the substrate was exposed to PEI. When the desorption time required to reach equilibrium was extended, the zigzag film growth disappeared and an alternate cycled assembly/disassembly pattern took its place. In the presence of a high-gravity field, the time-consuming Por desorption process using the conventional dipping LbL process can be remarkably accelerated by 30-fold, from 50 min to only 100 s, to reach the desorption equilibrium, which provides a convenient and simple method to investigate zigzag film growth behaviors.

■ ASSOCIATED CONTENT

Ⓢ Supporting Information

The Supporting Information is available free of charge on the ACS Publications website at DOI: 10.1021/acsami.5b05555.

Illustration of the high-gravity machine (PDF)

■ AUTHOR INFORMATION

Corresponding Author

*(F.S.) E-mail: shi@mail.buct.edu.cn.

Author Contributions

The manuscript was written through contributions of all authors. All authors have given approval to the final version of the manuscript.

Notes

The authors declare no competing financial interest.

■ ACKNOWLEDGMENTS

This work was supported by National Natural Science Foundation of China (21374006; 51422302), the Program of the Co-Construction with Beijing Municipal Commission of Education of China, Open Project of State Key Laboratory of Supramolecular Structure and Materials (SKLSSM2015017), and Beijing Young Talents Plan (YETP0488). We thank Dr. Dengli Qiu from Bruker (Beijing) Scientific Technology Co., Ltd., for his kind help with the AFM test and analysis.

■ REFERENCES

(1) Chia, K.-K.; Cohen, R. E.; Rubner, M. F. Amine-Rich Polyelectrolyte Multilayer Nanoreactors for in Situ Gold Nanoparticle Synthesis. *Chem. Mater.* **2008**, *20*, 6756−6763.

(2) Palomaki, P. K. B.; Civic, M. R.; Dinolfo, P. H. Photocurrent Enhancement by Multilayered Porphyrin Sensitizers in a Photoelectrochemical Cell. *ACS Appl. Mater. Interfaces* **2013**, *5*, 7604−7612.

(3) Li, H. L.; Pang, S. P.; Wu, S.; Feng, X. L.; Müllen, K.; Bubeck, C. Layer-by-Layer Assembly and UV Photoreduction of GraphenePolyoxometalate Composite Films for Electronics. *J. Am. Chem. Soc.* **2011**, *133*, 9423−9429.

(4) He, Q.; Möhwald, H.; Li, J. B. Layer-by-Layer Assembled Nanotubes as Biomimetic Nanoreactors for Calcium Carbonate Deposition. *Macromol. Rapid Commun.* **2009**, *30*, 1538−1542.

(5) Duan, L.; Yan, X. H.; Wang, A. H.; Jia, Y.; Li, J. B. Highly Loaded Hemoglobin Spheres as Promising Artificial Oxygen Carriers. *ACS Nano* **2012**, *6*, 6897−6904.

(6) Song, W. X.; He, Q.; Möhwald, H.; Yang, Y.; Li, J. B. Smart Polyelectrolyte Microcapsules as Carriers for Water-Soluble Small Molecular Drug. *J. Controlled Release* **2009**, *139*, 160−166.

(7) Wu, Y. J.; Lin, X. K.; Wu, Z. G.; Möhwald, H.; He, Q. Self-Propelled Polymer Multilayer Janus Capsules for Effective Drug Delivery and Light-Triggered Release. *ACS Appl. Mater. Interfaces* **2014**, *6*, 10476−10481.

(8) Tang, Z. Y.; Wang, Y.; Podsiadlo, P.; Kotov, N. A. Biomedical Applications of Layer-by-Layer Assembly: From Biomimetics to Tissue Engineering. *Adv. Mater.* **2006**, *18*, 3203−3224.

(9) Chen, S. S.; Li, X.; Li, Y.; Sun, J. Q. Intumescent Flame-Retardant and Self-Healing Superhydrophobic Coatings on Cotton Fabric. *ACS Nano* **2015**, *9*, 4070−4076.

(10) Fu, Y.; Chen, H.; Qiu, D. L.; Wang, Z. Q.; Zhang, X. Multilayer Assemblies of Poly(4-vinylpyridine) and Poly(acrylic acid) Bearing Photoisomeric Spironaphthoxazine via Hydrogen Bonding. *Langmuir* **2002**, *18*, 4989−4995.

(11) Li, L. D.; Tedeschi, C.; Kurth, D. G.; Möhwald, H. Synthesis of a Pyrene-Labeled Polyanion and Its Adsorption onto Polyelectrolyte Hollow Capsules Functionalized for Electron Transfer. *Chem. Mater.* **2004**, *16*, 570−573.

(12) Ochs, C. J.; Such, G. K.; Yan, Y.; van Koeverden, M. P.; Caruso, F. Biodegradable Click Capsules with Engineered Drug-Loaded Multilayers. *ACS Nano* **2010**, *4*, 1653−1663.

(13) Dai, Q.; Yan, Y.; Ang, C.-S.; Kempe, K.; Kamphuis, M. M. J.; Dodds, S. J.; Caruso, F. Monoclonal Antibody-Functionalized Multilayered Particles: Targeting Cancer Cells in the Presence of Protein Coronas. *ACS Nano* **2015**, *9*, 2876−2885.

(14) Das, S.; Pal, A. J. Layer-by-Layer Self-Assembling of a Low Molecular Weight Organic Material by Different Electrostatic Adsorption Processes. *Langmuir* **2002**, *18*, 458−461.

(15) Ariga, K.; Lvov, Y.; Kunitake, T. Assembling Alternate Dye−Polyion Molecular Films by Electrostatic Layer-by-Layer Adsorption. *J. Am. Chem. Soc.* **1997**, *119*, 2224−2231.

(16) Cheng, M. J.; Jiang, C.; Ding, Z. Y.; Zhang, Y. J.; Fu, Y.; Shi, F. Layer-by-Layer Self-Assembly and Disassembly of Single Charged Inorganic Small Molecules: Towards Surface Patterning. *Phys. Chem. Chem. Phys.* **2013**, *15*, 15172−15176.

(17) Min, J.; Braatz, R. D.; Hammond, P. T. Tunable Staged Release of Therapeutics from Layer-by-layer Coatings with Clay Interlayer Barrier. *Biomaterials* **2014**, *35*, 2507−2517.

(18) Chen, H.; Zeng, G. H.; Wang, Z. Q.; Zhang, X.; Peng, M.-L.; Wu, L. Z.; Tung, C.-H. To Combine Precursor Assembly and Layer-by-layer Deposition for Incorporation of Single-charged Species: Nanocontainers with Charge-selectivity and Nanoreactors. *Chem. Mater.* **2005**, *17*, 6679−6685.

(19) DeMuth, P. C.; Moon, J. J.; Suh, H.; Hammond, P. T.; Irvine, D. J. Releasable Layer-by-Layer Assembly of Stabilized Lipid Nanocapsules on Microneedles for Enhanced Transcutaneous Vaccine Delivery. *ACS Nano* **2012**, *6*, 8041−8051.

(20) Zhang, X.; Chen, H.; Zhang, H. Y. Layer-by-layer Assembly: from Conventional to Unconventional Methods. *Chem. Commun.* **2007**, 1395−1405.

(21) Schwarz, B.; Schönhoff, M. Surface Potential Driven Swelling of Polyelectrolyte Multilayers. *Langmuir* **2002**, *18*, 2964−2966.

(22) Wong, J. E.; Rehfeldt, F.; Hänni, P.; Tanaka, M.; Klitzing, R. V. Swelling Behavior of Polyelectrolyte Multilayers in Saturated Water Vapor. *Macromolecules* **2004**, *37*, 7285−7289.

(23) Carrière, D.; Krastev, R.; Schönhoff, M. Oscillations in Solvent Fraction of Polyelectrolyte Multilayers Driven by the Charge of the Terminating Layer. *Langmuir* **2004**, *20*, 11465−11472.

(24) Hoogeveen, N. G.; Stuart, M. A. C.; Fleer, G. J. Formation and Stability of Multilayers of Polyelectrolytes. *Langmuir* **1996**, *12*, 3675−3681.

(25) Kolarik, L.; Furlong, D. N.; Joy, H.; Struijk, C.; Rowe, R. Building Assemblies from High Molecular Weight Polyelectrolytes. *Langmuir* **1999**, *15*, 8265−8275.

(26) Tedeschi, C.; Caruso, F.; Möhwald, H.; Kirstein, S. Adsorption and Desorption Behavior of an Anionic Pyrene Chromophore in Sequentially Deposited Polyelectrolyte-Dye Thin Films. *J. Am. Chem. Soc.* **2000**, *122*, 5841−5848.

(27) Serizawa, T.; Kawanishi, N.; Akashi, M. Layer-by-Layer Assembly between Poly(vinylamine hydrochloride-co-N-vinylformamide) with Variable Primary Amine Content and Poly(sodium styrenesulfonate). *Macromolecules* **2003**, *36*, 1967−1974.

(28) Sui, Z. J.; Salloum, D.; Schlenoff, J. B. Effect of Molecular Weight on the Construction of Polyelectrolyte Multilayers: Stripping versus Sticking. *Langmuir* **2003**, *19*, 2491−2495.

(29) Micciulla, S.; Dodoo, S.; Chevigny, C.; Laschewsky, A.; von Klitzing, R. Short versus Long Chain Polyelectrolyte Multilayers: A Direct Comparison of Self-Assembly and Structural Properties. *Phys. Chem. Chem. Phys.* **2014**, *16*, 21988−21998.

(30) Ravati, S.; Favis, B. D. 3D Porous Polymeric Conductive Material Prepared Using LbL Deposition. *Polymer* **2011**, *52*, 718−731.

(31) Schwarz, B.; Schönhoff, M. Surface Potential Driven Swelling of Polyelectrolyte Multilayers. *Langmuir* **2002**, *18*, 2964−2966.

(32) Zou, Q. L.; Zhang, L.; Yan, X. H.; Wang, A. H.; Ma, G. H.; Li, J. B.; Möhwald, H.; Mann, S. Multifunctional Porous Microspheres Based on Peptide−Porphyrin Hierarchical Co-Assembly. *Angew. Chem., Int. Ed.* **2014**, *53*, 2366−2370.

(33) Liu, K.; Xing, R. R.; Chen, C. J.; Shen, G. Z.; Yan, L. Y.; Zou, Q. L.; Ma, G. H.; Möhwald, H.; Yan, X. H. Peptide-Induced Hierarchical Long-Range Order and Photocatalytic Activity of Porphyrin Assemblies. *Angew. Chem.* **2015**, *127*, 510−555.

(34) Chen, J. F.; Wang, Y. H.; Guo, F.; Wang, X. M.; Zheng, C. Synthesis of Nanoparticles with Novel Technology: High-Gravity Reactive Precipitation. *Ind. Eng. Chem. Res.* **2000**, *39*, 948−954.

(35) Ma, L. X.; Cheng, M. J.; Jia, G. J.; Wang, Y. Q.; An, Q.; Zeng, X. F.; Shen, Z. G.; Zhang, Y. J.; Shi, F. Layer-by-Layer Self-Assembly under High Gravity Field. *Langmuir* **2012**, *28*, 9849−9856.

(36) Liu, X. L.; Luo, C. J.; Jiang, C.; Shao, L.; Zhang, Y. W.; Shi, F. Rapid Multilayer Construction on Non-Planar Substrate by Layer-by-Layer Self-Assembly under High Gravity. *RSC Adv.* **2014**, *4*, 59528−59534.

(37) Jiang, C.; Liu, X. L.; Luo, C. J.; Zhang, Y. J.; Shao, L.; Shi, F. Controlled Exponential Growth in Layer-by-layer Multilayers Using High Gravity Fields. *J. Mater. Chem. A* **2014**, *2*, 14048−14053.

(38) Jiang, C.; Luo, C. J.; Liu, X. L.; Shao, L.; Dong, Y. Q.; Zhang, Y. W.; Shi, F. Adjusting the Ion Permeability of Polyelectrolyte Multilayers through Layer-by-Layer Assembly under a High Gravity Field. *ACS Appl. Mater. Interfaces* **2015**, *7*, 10920−10927.

DOI: 10.1021/acsami.5b05555